Webster, J.M., Ravelo, A.C., Grant, H.L.J., and the Expedition 389 Scientists
*Proceedings of the International Ocean Discovery Program* Volume 389
publications.iodp.org

# Site M0108[1]

J.M. Webster, A.C. Ravelo, H.L.J. Grant, M. Rydzy, M. Stewart, N. Allison, R. Asami, B. Boston, J.C. Braga, L. Brenner, X. Chen, P. Chutcharavan, A. Dutton, T. Felis, N. Fukuyo, E. Gischler, S. Greve, A. Hagen, Y. Hamon, E. Hathorne, M. Humblet, S. Jorry, P. Khanna, E. Le Ber, H. McGregor, R. Mortlock, T. Nohl, D. Potts, A. Prohaska, N. Prouty, W. Renema, K.H. Rubin, H. Westphal, and Y. Yokoyama[2]

[1] Webster, J.M., Ravelo, A.C., Grant, H.L.J., Rydzy, M., Stewart, M., Allison, N., Asami, R., Boston, B., Braga, J.C., Brenner, L., Chen, X., Chutcharavan, P., Dutton, A., Felis, T., Fukuyo, N., Gischler, E., Greve, S., Hagen, A., Hamon, Y., Hathorne, E., Humblet, M., Jorry, S., Khanna, P., Le Ber, E., McGregor, H., Mortlock, R., Nohl, T., Potts, D., Prohaska, A., Prouty, N., Renema, W., Rubin, K.H., Westphal, H., and Yokoyama, Y., 2025. Site M0108. In Webster, J.M., Ravelo, A.C., Grant, H.L.J., and the Expedition 389 Scientists, Hawaiian Drowned Reefs. Proceedings of the International Ocean Discovery Program, 389: College Station, TX (International Ocean Discovery Program). https://doi.org/10.14379/iodp.proc.389.115.2025

[2] **Expedition 389 Scientists' affiliations.**

**Contents**



**Keywords**
International Ocean Discovery Program, IODP, Expedition 389, *MMA Valour*, Hawaiian Drowned Reefs, Earth climate system, Earth system feedbacks, Earth history tipping points, Site M0108, coral reef, volcanics, sea level, paleoclimate, central Pacific, reef health, Hawaiian geology, basalt, lava, carbonates, Mahukona

**Core descriptions**

**Supplementary material**

**References (RIS)**

**MS 389-115**
Published 26 February 2025

Funded by ECORD, JAMSTEC, and NSF OCE1326927

## 1. Operations

The multipurpose vessel *MMA Valour* was used as the drilling platform throughout Expedition 389. At all Expedition 389 sites, dynamic positioning was used to provide accurate positions throughout operations and water depth was established using a Sound Velocity Profiler (SVP) placed on the top of the PROD5 drilling system. For more detail on acquisition methods, see **Introduction** in the Expedition 389 methods chapter (Webster et al., 2025a).

Summary operational information for Site M0108 is provided in Table **T1**. All times stated are in Hawaiian Standard Time (HST).

### 1.1. Hole M0108A

The *MMA Valour* arrived on location at 0830 h on 24 October 2023. PROD5 was deployed at 1100 h at a water depth of 1178.4 m. Rotary coring and casing commenced in difficult-to-drill lithologies, which meant coring progress was slow. At 1512 h and 2.05 meters below seafloor (mbsf), PROD5 had an oil leak on the top drive and was recovered to deck for repairs at 1610 h on 24 October. On-deck operations commenced, core barrels were extracted for curation, and repairs were undertaken.

A total of six cores were recovered from Hole M0108A from 1.97 m of rotary coring. The total core recovered length was 1.95 m (98.98% recovery).

### 1.2. Hole M0108B

PROD5 was redeployed after repairs at 1745 h on 24 October 2023 at a water depth of 1177.2 m, approximately 2 m away from Hole M0108A. Coring and casing commenced in Hole M0108B at

**Table T1.** Hole summary, Site M0108. R = rotary coring mode, W = wash down mode. LAT = Lowest Astronomical Tide. **Download table in CSV format.**

| Hole | Water depth (mbsf) | Date started (2023) | Date finished (2023) | Latitude | Longitude | Coring method | Total drilled depth (m) | Recovered length (m) | Core recovery (%) | Cores (*N*) | Notes |
|---|---|---|---|---|---|---|---|---|---|---|---|
| 389-M0108A | 1178.4 | 24 Oct | 24 Oct | 20.048364° | −156.192745° | R | 1.97 | 1.95 | 99 | 6 | LAT water depth: 1177.8 m. Borehole terminated due to technical issues. |
| M0108B | 1177.2 | 24 Oct | 26 Oct | 20.048346° | −156.192127° | W; R | 30.70 | 16.35 | 63 | 33 | LAT water depth: 1176.6 m. Washed to 1.86 m. Maximum quantity of barrels was achieved. |

1916 h with wash boring to 2 m, approximately the final depth of Hole M0108A. Difficult gravelly lithology and hole conditions similar to those in Hole M0108A were encountered. Because of a lack of coring advancement and material blockages causing very short runs, at 0142 h on 25 October the decision was made to wash bore to 7.50 mbsf and clean the hole to see if this helped. Rotary coring commenced again at 0512 h with two more intervals of wash boring through difficult ground at 10.40–11.55 and 20.13–21.75 mbsf. Coring advanced to 30.84 mbsf at 2035 h on 26 October, when all core barrels were utilized, and PROD5 was recovered to deck at 2203 h. On-deck operations commenced, and core barrels were extracted for curation. The transit to Site M0109 began at 2223 h on 26 October.

A total of 33 cores were recovered from Hole M0108B from 25.82 m of rotary coring (4.88 m wash bore). The total recovered core length was 16.35 m (63.32% recovery).

## 2. Lithostratigraphy

Holes M0108A and M0108B are located on the same subterrace in the Kawaihae region, at 1178.4 m and 1177.2 meters below sea level (mbsl), respectively (Figure **F1**). Based on the main facies changes, three main lithostratigraphic intervals are identified:

- Interval 1, spanning all of Hole M0108A to its base at 2.27 mbsf, and the upper part of Hole M0108B (1.86–8.83 mbsf; no recovery above), is dominated by coralgal-microbialite boundstone with robust branching *Porites*.
- Interval 2, recovered only in Hole M0108B from 8.83 to 25.25 mbsf, is composed predominantly of highly fragmented coralgal boundstone embedded locally in a biodetrital matrix.
- Interval 3, from 25.25 mbsf to the base of Hole M108B at 30.70 mbsf, consists mostly of an unconsolidated coarse-grained biodetrital sediment with abundant loose reworked large *Porites* and *Montipora* clasts, as well as crustose coralline algae (CCA) fragments.

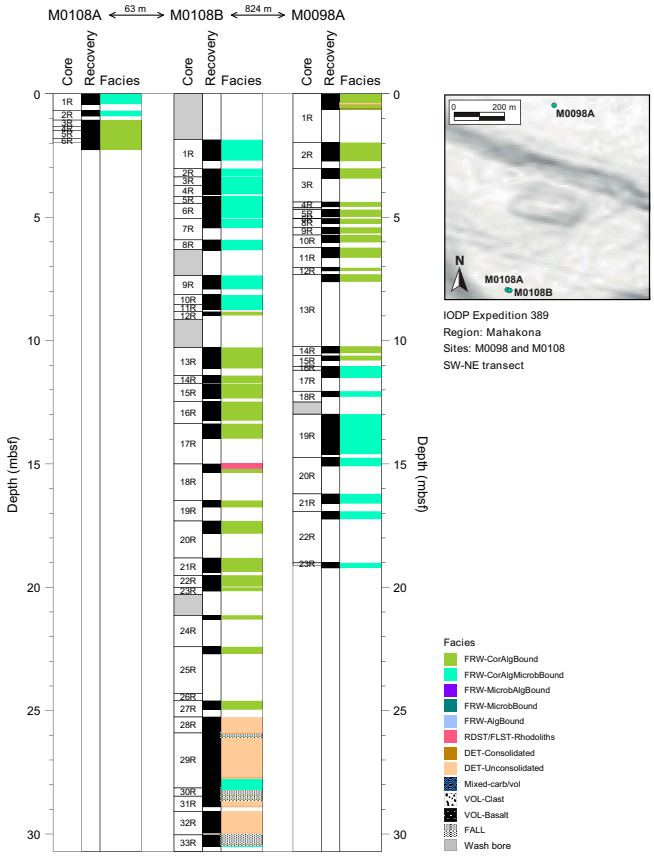


**Figure F1.** Lithostratigraphy, Holes M0108A and M0108B.

## 2.1. Hole M0108A

Hole M0108A (Figure F2) is composed of highly fragmented (due to coring disturbance) coralgal-microbialite boundstone from 0.00 to 1.06 mbsf and contains robust branching *Porites*, which are bioeroded and encrusted with thin CCA and subsequently with structureless microbialite (Figure F3A). Loose mollusk fragments and echinoid spines are present as unbound components within the fragmented material.

From 1.06 mbsf to the base of the hole at 2.27 mbsf, coring disturbance is high and the lithology consists of fragments of coralgal boundstone composed of robust branching and laminar *Porites* encrusted with centimeter-thick CCA crusts (Figure F3B). Some corals are bored, with borings partially filled with sediment.

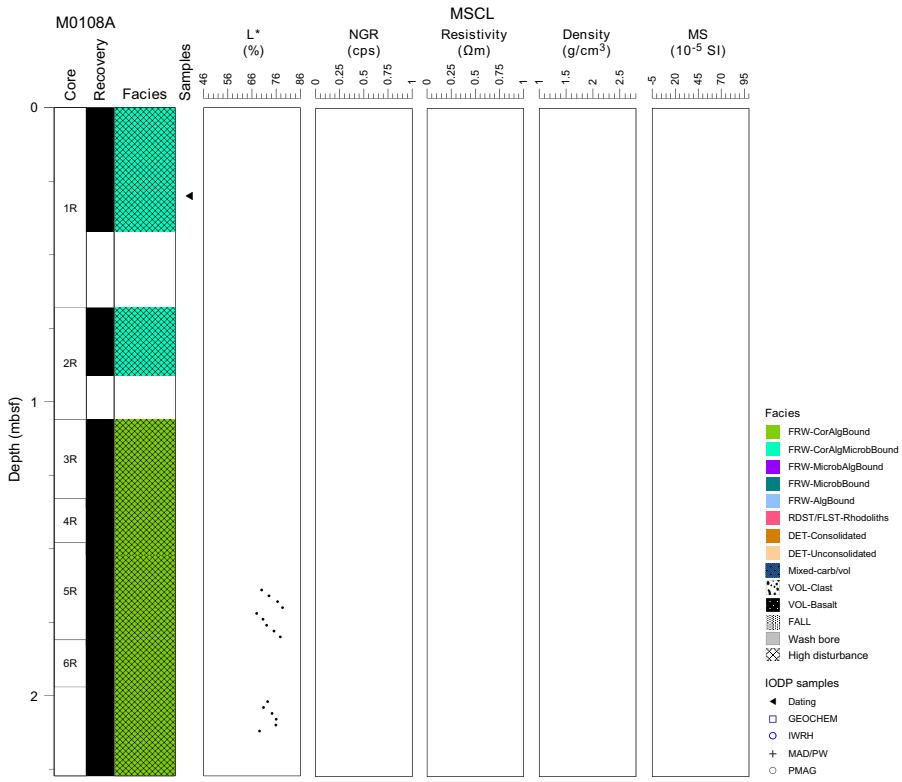


**Figure F2.** Lithostratigraphy and MSCL data, Hole M0108A. cps = counts per second, NGR = natural gamma radiation, MS = magnetic susceptibility. MSCL data were not acquired due to extensive drilling-induced core damage.

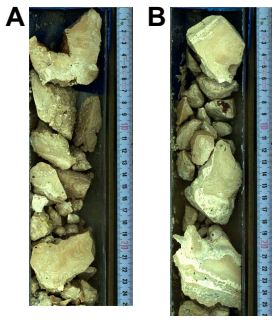


**Figure F3.** Lithologies, Hole M0108A. A. Highly disturbed coralgal-microbialite boundstone consisting of bored, robust *Porites* branches encrusted with thin CCA and structureless microbialite (1R-1, 0–25 cm). B. Fragments of coralgal boundstone consisting of pieces of robustly branching and laminar *Porites* encrusted with centimeter-thick CCA crusts (5R-1, 0–26 cm).

## 2.2. Hole M0108B

There was no recovery in Hole M0108B (Figure **F4**) from 0.00 to 1.86 mbsf because the hole was initially wash bored. Heavily fragmented coralgal-microbialite boundstone from 1.86 to 8.83 mbsf is dominated by robust branching *Porites* that are bioeroded and encrusted with thin CCA, which are in turn covered with structureless microbialite crusts (Figure **F5A**). Laminar *Cyphastrea* and clasts of *Montipora* are also present. In this interval (3.37–5.01 mbsf), fragments of the reef framework are embedded in an unconsolidated, medium- to coarse-grained biodetrital matrix (Figure **F5B**) containing gastropods, bivalves, and large benthic foraminifers.

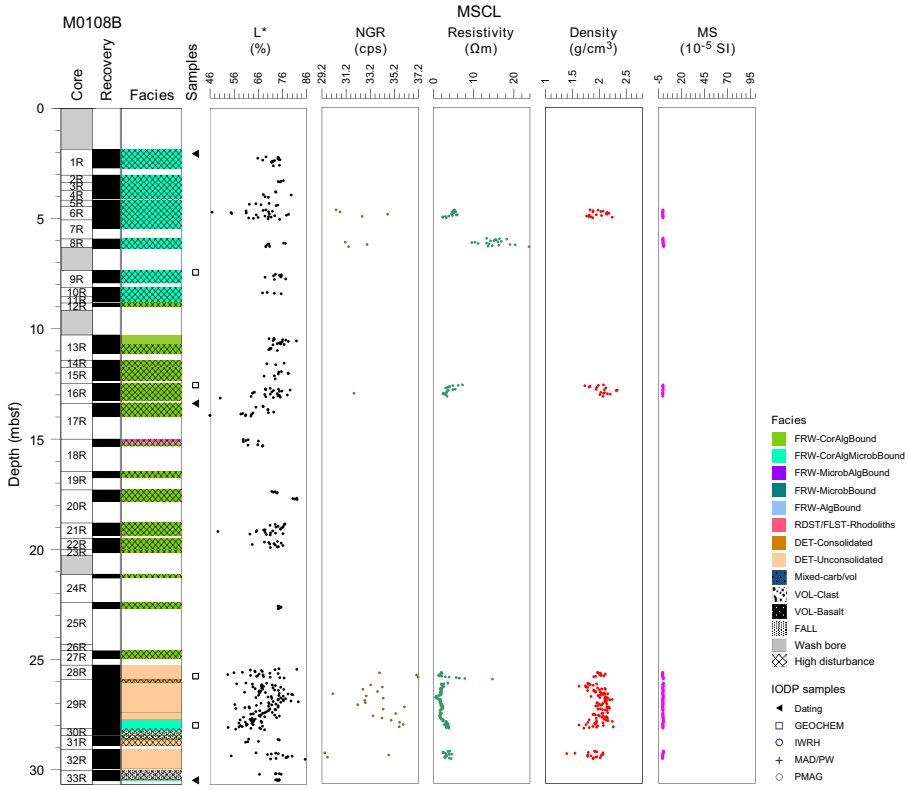


**Figure F4.** Lithostratigraphy and MSCL data, Hole M0108B. cps = counts per second, NGR = natural gamma radiation, MS = magnetic susceptibility.

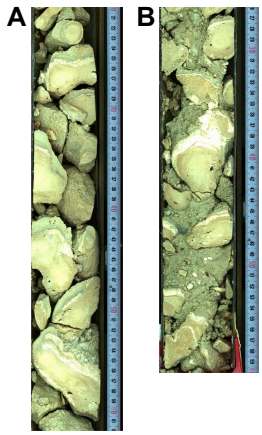


**Figure F5.** Coral, Hole M0108B. A. Coralgal-microbialite boundstone dominated by robust branching, bioeroded *Porites* encrusted with thin CCA and thicker structureless microbialite (1R-1, 20–62 cm). B. Fragments of coralgal-microbialite boundstone embedded in an unconsolidated, medium- to coarse-grained biodetrital matrix containing gastropods, bivalves, and large benthic foraminifers (6R-1, 26–60 cm).

From 8.83 to 25.25 mbsf, a thick succession of highly fragmented (coring disturbance) coralgal boundstone is interrupted by a thin interval of rhodoliths (possible fall in?) between 15.00 and 15.15 mbsf (Figure **F6A**). Recovered material consists predominantly of fragmented, robust branching *Porites* and rare submassive *Porites* that are bioeroded and thinly encrusted with CCA (Figure **F6B**). From 10.72 to 15.00 mbsf and from 18.81 to 19.97 mbsf, these coral fragments are embedded in an unconsolidated biodetrital matrix containing bivalves, gastropods, CCA, corals, and echinoid spines.

From 25.25 mbsf to the base of the hole at 30.70 mbsf, the lithology is composed predominantly of loose, reworked, large coral and CCA fragments in an unconsolidated coarse-grained biodetrital matrix (Figure **F6C**). The coral fragments are identified as *Porites* branches, platy *Montipora*, and less abundant encrusting *Cyphastrea*. They are in many cases encrusted with thin CCA crusts, interlayered with vermetids and *Homotrema*, followed by very thin structureless microbialite. The biodetrital matrix consists of gastropods, bivalves, coral debris, and algal debris and locally includes centimeter-scale rhodoliths. This interval is interrupted from 27.72 to 28.21 mbsf by a possible in situ coralgal-microbialite boundstone (Figure **F7**) composed of altered, platy, and branching *Montipora* with thin CCA encrustation followed by thin structureless microbialite crusts. The biodetrital matrix fills framework cavities.

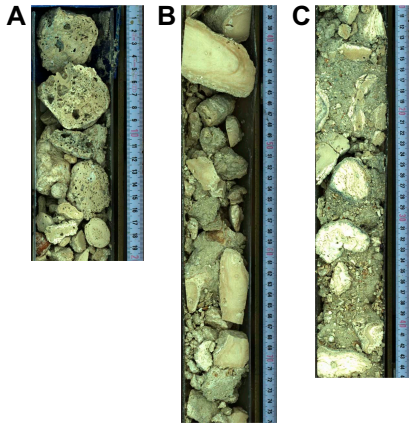


**Figure F6.** Lithologies, Hole M0108B. A. Rhodoliths (possible fall in?) (18R-1, 0–20 cm). B. Fragmented, robust branching, bioeroded *Porites*, thinly encrusted with CCA (13R-1, 37–76 cm). C. Large, loose, reworked coral and CCA fragments in an unconsolidated coarse-grained biodetrital matrix (32R-1, 10–45 cm).

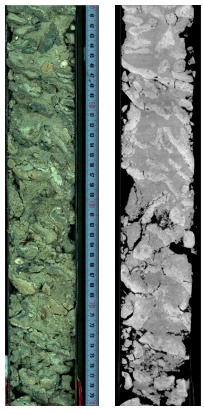

**Figure F7.** Lithologies, Hole M0108B. Possible in situ coralgal-microbialite framework composed of altered, platy, and branching *Montipora* encrusted with thin CCA followed by thin structureless microbialite crusts (29R-2, 40–80 cm). Left: high-resolution linescan image. Right: X-ray computed tomography scan image (orthogonal view 0°).

# 3. Physical properties

Physical properties data for Site M0108 are shown in Table **T2** in the Site M0096 chapter (Webster et al., 2025b).

## 3.1. Hole M0108A

Because of the poor quality (drilling disturbance) of the core material, none of the cores from Hole M0108A were scanned with the multisensor core logger (MSCL) and no discrete samples were taken for *P*-wave velocity and moisture and density (MAD) measurements. Digital linescans, color reflectance, and hyperspectral imaging were acquired on all cores.

### 3.1.1. Digital linescans, color reflectance, and hyperspectral imaging

All cores from Hole M0108A were digitally scanned, and, where appropriate, measured for color reflectance and imaged with the hyperspectral scanner (see HYPERSPECTRAL in **Supplementary material**). Color reflectance L* values vary between 67.92% and 78.66%, a* varies between 0.39 and 1.97, b* varies between 11.51 and 18.60, and a*/b* varies between 0.03 and 0.11 (Figure **F2**). Color reflectance data coverage was too sparse to observe whether any downhole trends were present in the data.

## 3.2. Hole M0108B

A total of 12.78 m of core from Hole M0108B was scanned with the MSCL, and because the core exhibited major drilling-induced disturbance, only 31% of the acquired data passed QA/QC (see Table **T10** in the Expedition 389 methods chapter [Webster et al., 2025a]). No discrete samples were taken for *P*-wave velocity and MAD measurements because there was no suitable core material. Digital linescans, color reflectance, and hyperspectral imaging were acquired on all cores.

### 3.2.1. Density and porosity

Data for density and porosity measurements are presented in Figure **F4**. MSCL bulk density measurements range 1.39–2.33 g/cm$^3$. The core disturbance and the short core lengths compromised data quality (see **Physical properties** in the Expedition 389 methods chapter [Webster et al., 2025a]) and prohibited sampling.

### 3.2.2. *P*-wave velocity

MSCL *P*-wave velocity measurements yielded no data, and it was not possible to collect discrete *P*-wave samples because of the unconsolidated nature of the core material.

### 3.2.3. Thermal conductivity

It was not possible to measure samples for thermal conductivity measurements because of the unconsolidated nature of the core material.

### 3.2.4. Magnetic susceptibility

MSCL magnetic susceptibility data range $-0.67 \times 10^{-5}$ to $0.60 \times 10^{-5}$ SI (Figure **F4**) with mean values close to $-0.23 \times 10^{-5}$ SI. There is no apparent trend in the data.

### 3.2.5. Electrical resistivity

MCSL noncontact resistivity measurements range 0.62–23.74 Ωm (Figure **F4**). Similar to other data sets for this hole, there are no apparent trends or notable features.

### 3.2.6. Natural gamma radiation

MCSL natural gamma radiation measurements range 29–37 counts/s (Figure **F4**) and show no apparent downhole change.

### 3.2.7. Digital linescans, color reflectance, and hyperspectral imaging

All cores from Hole M0108B were digitally scanned, and, where appropriate, measured for color reflectance and imaged with the hyperspectral scanner (see HYPERSPECTRAL in **Supplemen-**

tary material). Color reflectance L* values vary between 43.97% and 82.37%, a* varies between −1.02 and 3.87, b* varies between 6.49 and 19.92, and a*/b* varies between −0.13 and 0.28 (Figure F4). There are no apparent trends in color reflectance, although there is a wider range of values in the unconsolidated sediment units near the base of the hole.

# 4. Geochemistry

## 4.1. Interstitial water

No interstitial water samples were collected from Site M0108.

## 4.2. Surface seawater

One surface seawater sample was collected from Site M0108 using a Niskin bottle deployed from the side of the vessel (see Figure F22 in the Expedition 389 methods chapter [Webster et al., 2025a]). The salinity, pH, alkalinity, and ammonium concentration were analyzed off shore, and major cations and anions were measured during the Onshore Science Party. The salinity, pH, alkalinity, ammonium, and major element chemistry measured for the Site M0108 seawater sample are consistent with the other surface seawater samples taken during Expedition 389 and align with the expected values for conservative elements in seawater (see Tables T15 and T17 in the Expedition 389 methods chapter [Webster et al., 2025a]).

## 4.3. Bulk sediment and rocks

Four bulk sediments were taken from Hole M0108B (Figure F5) and analyzed for mineralogy and elemental composition. The sample facies (see Figure F10 in the Expedition 389 methods chapter [Webster et al., 2025a]) are coralgal-microbialite boundstone, coralgal boundstone, and coral and CCA fragments (Figure F5).

## 4.4. Mineralogy

Samples from Site M0108 contain primarily carbonate minerals, primarily aragonite (43%–58%) and Mg-rich calcite (35%–47%) (Table T2). The samples also contain calcite (6%–8%), except for Sample 389-M0108B-29R-2, 58.5–60.5 cm (27.99 mbsf), from the coral and CCA fragment facies, which only contains Mg-rich calcite (40%), aragonite (58%), and sulfides (2%), reported as 2 wt% copper sulfide (covellite).

## 4.5. Elemental abundances

The concentrations of major elements in bulk sediment and rock samples from Site M0108 are consistent with the carbonate lithologies of the samples (Table T3). Calcium concentrations in the samples are high and range 340,945–362,823 mg/kg (for comparison, pure $CaCO_3$ has 400,000 mg/kg Ca). From 25.25 to 30.70 mbsf, the lithology is dominated by coral and CCA (Figure F5), and the two bulk samples from this interval contain slightly lower Mg (26,413 and 27,967 mg/kg) and slightly higher Sr (4,299 and 4,476 mg/kg) concentrations compared to the coralgal and coralgal-microbialite boundstone lithologies (Mg = 30,412 and 32,061 mg/kg; Sr = 4,049 and 3,125 mg/kg) (Table T3). Other elements analyzed are either minor in concentration or below detection limits.

**Table T2.** HighScore X-ray diffraction (XRD) mineral abundances, Site M0108. **Download table in CSV format.**

**Table T3.** Solid-phase elemental abundances, Site M0108. **Download table in CSV format.**

**Table T4.** TOC, TIC, and TC, Site M0108. **Download table in CSV format.**

## 4.6. Carbon content

The results for total organic carbon (TOC), total carbon (TC), and total inorganic carbon (TIC) at Site M0108B are presented in (Table T4). TC content ranges 11.4%–11.6%, TOC ranges 0.18%–0.26%, and TIC ranges 11.2%–11.4%, which calculates to a $CaCO_3$ content of 93%–95%. These results are consistent with the carbonate lithologies from which these samples were collected.

# 5. Paleomagnetism

Because the recovered core lithologies were not suitable for sampling, no samples were analyzed for paleomagnetic properties for Site M0108.

# 6. Geochronology

Four samples were U-Th dated for Site M0108 (see Tables T21 and T22 in the Expedition 389 methods chapter [Webster et al., 2025a]). The topmost sample from Hole M0108A (1R-1, 30–32 cm) is rejected based on an anomalously high $^{238}U$ concentration (>4 ppm) and an anomalously high $\delta^{234}U$ initial value (>160‰). The remaining three samples from Hole M0108B provide dates ranging ~364–472 ky BP, although the lower two samples (17R-1, 2–4 cm, and 33R-1, 45–47 cm) reveal a stratigraphic age reversal. Although not specifically discussed in Webster et al. (2009), these dates are consistent with the timing of stratigraphically adjacent terraces in that paper and with the ages and depths of dated corals in Ludwig et al. (1991).

# References

Ludwig, K.R., Szabo, B.J., Moore, J.G., and Simmons, K.R., 1991. Crustal subsidence rate off Hawaii determined from $^{234}U/^{238}U$ ages of drowned coral reefs. Geology, 19(2):171–174. **https://doi.org/10.1130/0091-7613(1991)019<0171:CSROHD>2.3.CO;2**

Webster, J.M., Braga, J.C., Clague, D.A., Gallup, C., Hein, J.R., Potts, D.C., Renema, W., Riding, R., Riker-Coleman, K., Silver, E., and Wallace, L.M., 2009. Coral reef evolution on rapidly subsiding margins. Global and Planetary Change, 66(1–2):129–148. **https://doi.org/10.1016/j.gloplacha.2008.07.010**

Webster, J.M., Ravelo, A.C., Grant, H.L.J., and the Expedition 389 Scientists, 2025. Supplementary material, **https://doi.org/10.14379/iodp.proc.389supp.2025**. In Webster, J.M., Ravelo, A.C., Grant, H.L.J., and the Expedition 389 Scientists, Hawaiian Drowned Reefs. Proceedings of the International Ocean Discovery Program, 389: College Station, TX (International Ocean Discovery Program).

Webster, J.M., Ravelo, A.C., Grant, H.L.J., Rydzy, M., Stewart, M., Allison, N., Asami, R., Boston, B., Braga, J.C., Brenner, L., Chen, X., Chutcharavan, P., Dutton, A., Felis, T., Fukuyo, N., Gischler, E., Greve, S., Hagen, A., Hamon, Y., Hathorne, E., Humblet, M., Jorry, S., Khanna, P., Le Ber, E., McGregor, H., Mortlock, R., Nohl, T., Potts, D., Prohaska, A., Prouty, N., Renema, W., Rubin, K.H., Westphal, H., and Yokoyama, Y., 2025a. Expedition 389 methods. In Webster, J.M., Ravelo, A.C., Grant, H.L.J., and the Expedition 389 Scientists, Hawaiian Drowned Reefs. Proceedings of the International Ocean Discovery Program, 389: College Station, TX (International Ocean Discovery Program). **https://doi.org/10.14379/iodp.proc.389.102.2025**

Webster, J.M., Ravelo, A.C., Grant, H.L.J., Rydzy, M., Stewart, M., Allison, N., Asami, R., Boston, B., Braga, J.C., Brenner, L., Chen, X., Chutcharavan, P., Dutton, A., Felis, T., Fukuyo, N., Gischler, E., Greve, S., Hagen, A., Hamon, Y., Hathorne, E., Humblet, M., Jorry, S., Khanna, P., Le Ber, E., McGregor, H., Mortlock, R., Nohl, T., Potts, D., Prohaska, A., Prouty, N., Renema, W., Rubin, K.H., Westphal, H., and Yokoyama, Y., 2025b. Site M0096. In Webster, J.M., Ravelo, A.C., Grant, H.L.J., and the Expedition 389 Scientists, Hawaiian Drowned Reefs. Proceedings of the International Ocean Discovery Program, 389: College Station, TX (International Ocean Discovery Program). **https://doi.org/10.14379/iodp.proc.389.103.2025**